

# Steric Molecular Combing Effect Enables Ultra-Fast Self-Healing Electrolyte in Quasi- Solid-State Zinc-Ion Batteries

*Qin Liu<sup>1</sup>, Renpeng Chen<sup>1</sup>, Lin Xu<sup>1,2\*</sup>, Yu Liu<sup>1</sup>, Yuhang Dai<sup>1</sup>, Meng Huang<sup>1</sup>, and  
Liqiang Mai<sup>1,2\*</sup>*

<sup>1</sup> State Key Laboratory of Advanced Technology for Materials Synthesis and Processing, School of Materials Science and Engineering, Wuhan University of Technology, Wuhan 430070, Hubei, P. R. China

<sup>2</sup> Foshan Xianhu Laboratory of the Advanced Energy Science and Technology Guangdong Laboratory, Xianhu Hydrogen Valley, Foshan 528200, Guangdong, P. R. China

**Corresponding Author**

\*E-mail: [linxu@whut.edu.cn](mailto:linxu@whut.edu.cn) (Lin Xu); [mlq518@whut.edu.cn](mailto:mlq518@whut.edu.cn) (Liqiang Mai).

## Experimental section

*Preparation of the cathode:* The  $\text{MnO}_2$  nanoballs were prepared by a facile hydrothermal method. Briefly, 1mmol  $\text{KMnO}_4$  and 1mmol  $\text{Zn}(\text{NO}_3)_2 \cdot 6\text{H}_2\text{O}$  were dissolved in 75 mL deionized water under stirring. The carbon cloth (2 cm\*2 cm) was soaked in nitric acid and then cleaned with deionized water. Subsequently, the suspension and carbon cloth were transferred into a 100 mL Teflon-lined stainless steel autoclave and heated at 140°C for 3.5 h. The final precipitate attached on carbon cloth was peeled off and washed with deionized water and ethanol for each three times by centrifuge. Finally, the  $\text{MnO}_2$  nanoball powders were obtained after drying under vacuum at 70°C for 24 h.

*Preparation of electrolyte:* 1 ml glycerol was added into the 10 mL 1M  $\text{ZnSO}_4$  solution. Then, 0.6 g guar gum (Aladdin) was added to the as-prepared binary system solution (AR grade, Macklin) under stirring at room temperature until the guar gum was dissolved. Subsequently, add 0.5 ml neutral organic boron crosslinker drop by drop while stirring with a glass rod. After solidification, guar gum/ $\text{ZnSO}_4$ /glycerol ultra-fast electrolyte was obtained. The preparation method of the guar gum/ $\text{ZnSO}_4$  electrolyte is similar to that of ultra-fast electrolyte; however, no glycerol is introduced during the synthesis process.

For comparison, 0.8 ml and 1.2 ml glycerol were added into the 10 mL 1M  $\text{ZnSO}_4$  solution, respectively. The subsequent steps are consistent with the above operations to explore the effect of glycerol content on electrolyte performance. These two

electrolytes are named guar gum/ZnSO<sub>4</sub>/glycerol-0.8 ml and guar gum/ZnSO<sub>4</sub>/glycerol-1.2 ml

*Preparation of the full cells:* To fabricate the full batteries, where MnO<sub>2</sub> nanoballs acted as cathode electrode and Zn foil acted as anode electrode. The cathode electrode of MnO<sub>2</sub> was prepared by mixing 70% active materials, 20% conductive acetylene black and 10% polyvinylidene fluoride (PVDF). Then, the slurries were coated onto the Ti foil. The mass loading of MnO<sub>2</sub> was ~1.5 mg cm<sup>-2</sup>. Guar gum/ZnSO<sub>4</sub>/glycerol, guar gum/ZnSO<sub>4</sub> and 1 M ZnSO<sub>4</sub> solution were prepared as the electrolyte, separately.

*Characterizations:* The optical images of the electrolyte and the in-situ observation were recorded by optical microscopy (Sunny Optics, 50/100× objective). Scanning electron microscope (SEM) measurement was taken on by a JEOL JSM-7100F with 20 kV acceleration voltage. Fourier Transform Infrared Spectrometer (FTIR) spectra were measured the FTIR spectrometer (Nicolet, Magna IR 560).

*Electrochemical Measurements:* Electrochemical measurements data were performed with an Autolab PGSTAT302N electrochemical workstation. The long-term cycling performance of the full batteries and the Zn//Zn symmetrical cells was conducted using a LAND CT2001A multichannel testing system.

*Density functional theory calculations:* All density functional theory (DFT) calculations were carried out using the Dmol3 program applied in the Materials Studio 7.0 software package. The exchange-correlation was Perdew-Burke-Ernzerhof (PBE) functional

with the formulation of generalized gradient approximation (GGA)<sup>1</sup> and the basis set was DNP. The Max. force and Max. displacement is about 0.002 Ha/Å and 0.005 Å, respectively.

The adsorption energies ( $\Delta E_{\text{ads}}$ ) of molecules (H<sub>2</sub>O and C<sub>3</sub>) on adsorbent (M) are calculated by the following equation:

$$\Delta E_{\text{ads}} = E_{\text{molecule/M}} - E_{\text{molecule}} - E_{\text{M}},$$

where  $E_{\text{molecule/M}}$ ,  $E_{\text{molecule}}$  and  $E_{\text{M}}$  are total energies of the adsorbed molecule, the free molecule and M from DFT calculations, respectively. According to this formula, the more negative  $\Delta E_{\text{ads}}$  value, the stronger the adsorption capacity.

### *Molecular dynamics simulations*

The guar molecule consisting of 3 monomers was first constructed, and thereafter quantum chemistry calculations were performed to optimize its molecular geometry using the Gaussian 16 package<sup>2</sup> at B3LYP/6-311+G(d,p) level of theory. The atomic partial charges on guar gum molecule were calculated using the ChelpG method at the same level of theory (the B3LYP hybrid functional and the 6-311+G(d,p) basis set). The atomistic force field parameters for Zn and sulfate are described by AMBER format<sup>3</sup>. The SPC/E water model was adopted in the current work. The cross-interaction parameters between different atom types are obtained from the Lorentz-Berthelot combination rule.

Atomistic simulations were performed using the GROMACS package with cubic periodic boundary conditions<sup>4</sup>. The modelling system containing glycerol molecules are consisting of 88 ZnSO<sub>4</sub>, 25 guar gum molecules and 110 glycerol molecules dispersed in 4400 water molecules, and the reference modelling system without glycerol molecules follow the same chemical compositions. The equations of motion of all atoms were integrated using a classic Verlet leapfrog integration algorithm with a time step of 1.0 fs. A cutoff radius of 1.6 nm was set for short-range van der Waals interactions and real-space electrostatic interactions. The particle-mesh Ewald (PME) summation method with an interpolation order of 5 and a Fourier grid spacing of 0.20 nm was employed to handle long range electrostatic interactions in reciprocal space. All simulation systems were first energetically minimized using a steepest descent algorithm, and thereafter annealed gradually from 600 K to room temperature (300 K) within 10 ns. All annealed simulation systems were equilibrated in an isothermal-isobaric (NPT) ensemble for 20 ns of physical time maintained using a Nosé-Hoover thermostat and a Parrinello-Rahman barostat with time coupling constants of 0.4 and 0.2 ps, respectively, to control the temperature at 300 K and the pressure at 1 atm. Atomistic simulations were further performed in a canonical ensemble (NVT) for 40 ns, and simulation trajectories were recorded at an interval of 100 fs for further structural and dynamical analysis.

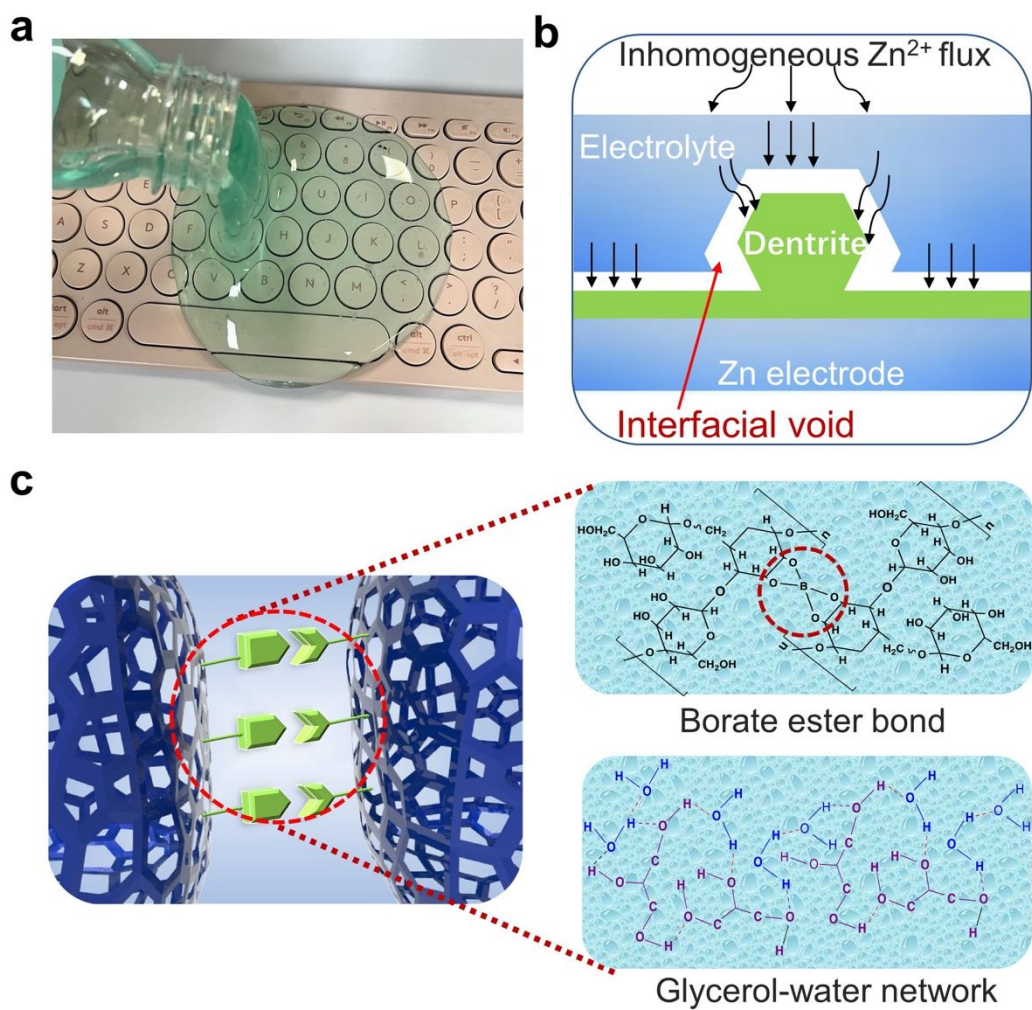


Figure S1 Design of guar gum-based self-healing electrolyte. (a) Digital picture of commercial “art water”. (b) Schematic of interfacial separation problem caused during conventional Zn plating/stripping process. (c) Schematic for the structure of the designed guar gum-based self-healing electrolyte: guar gum/ $ZnSO_4$ /glycerol.

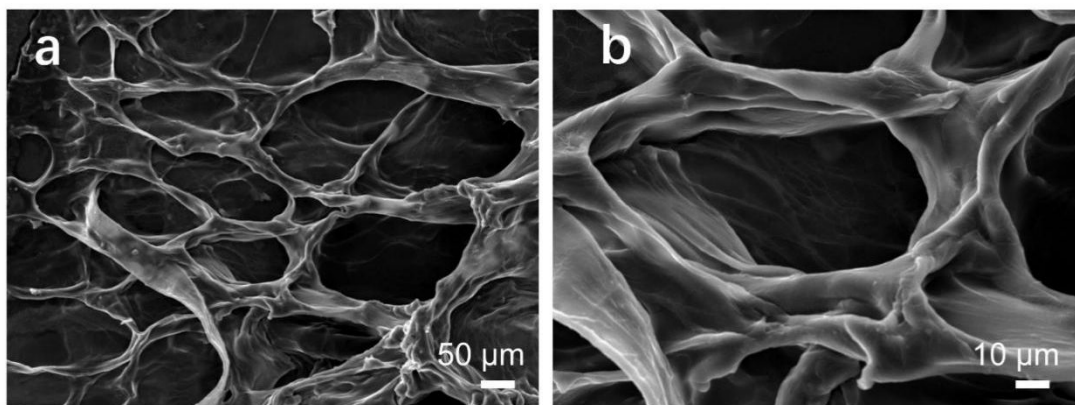


Figure S2 SEM images of the guar gum-based electrolyte. The guar gum/ $\text{ZnSO}_4$ /glycerol electrolyte after freeze-drying with (a) low magnification and (b) high magnification.

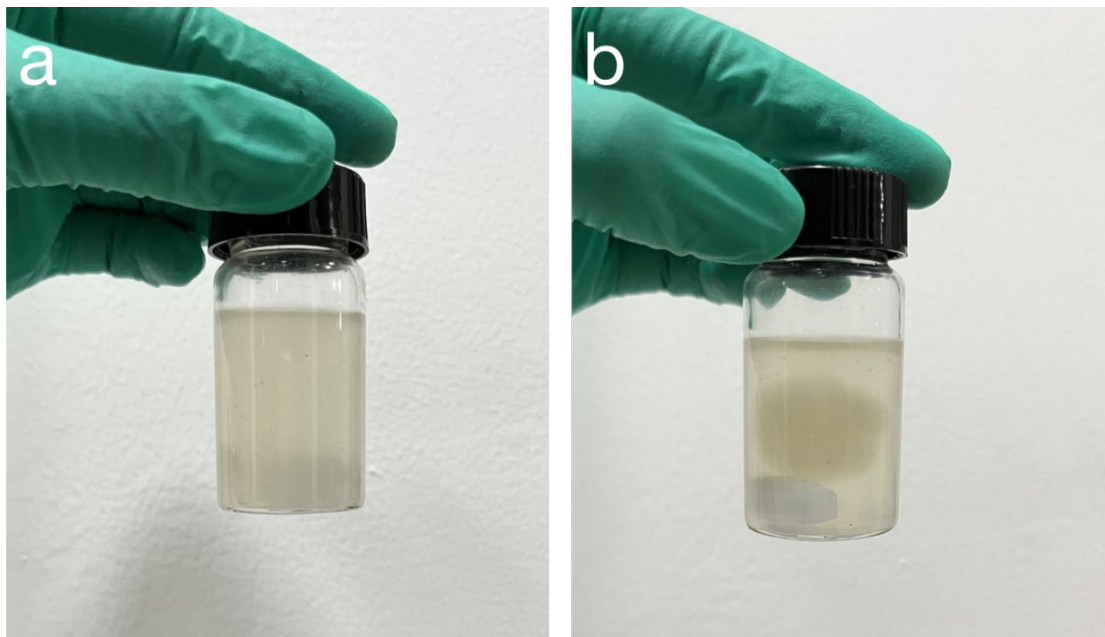


Figure S3 The optical photographs of different electrolytes before cross-linking. (a) guar gum/ $\text{ZnSO}_4$ /glycerol system (b) guar gum/ $\text{ZnSO}_4$  system.

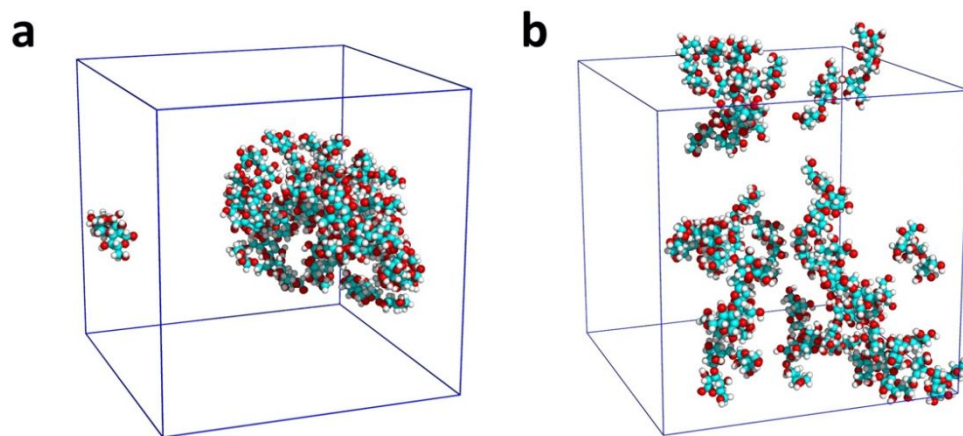


Figure S4 3D snapshot of guar gum obtained from MD simulations. (a) guar gum/ $\text{ZnSO}_4$  system (b) guar gum/ $\text{ZnSO}_4$ /glycerol system.

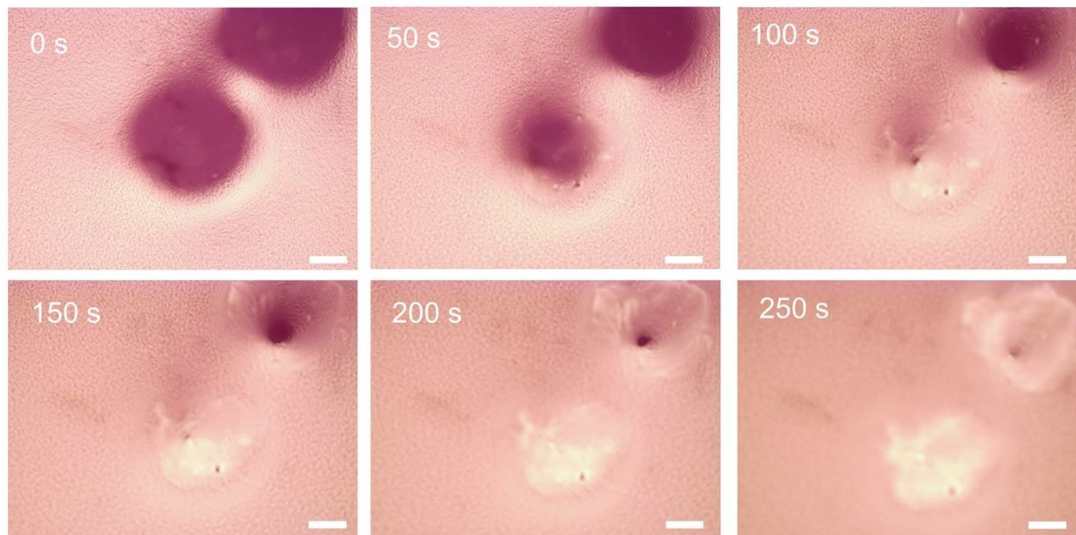


Figure S5 Optical images of the self-healing process of the guar gum-based electrolyte.

Guar gum/ $\text{ZnSO}_4$ /glycerol-0.8 mL electrolyte can realize self-healing within 250 s.

Scale bars: 10  $\mu\text{m}$ .

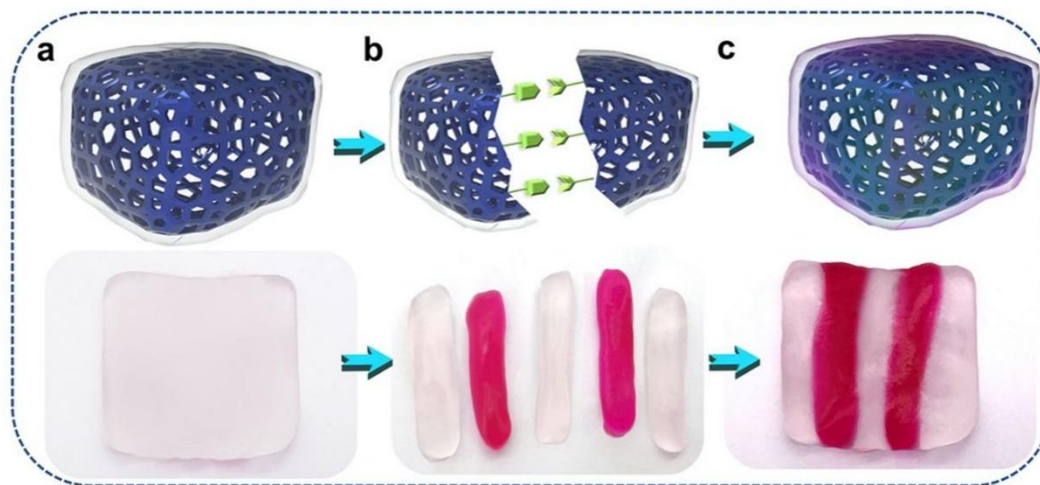


Figure S6 The self-healing behavior of the guar gum/ $\text{ZnSO}_4$ /glycerol electrolyte. (a)

Before cutting. (b) Cutting-off. (c) After self-healing

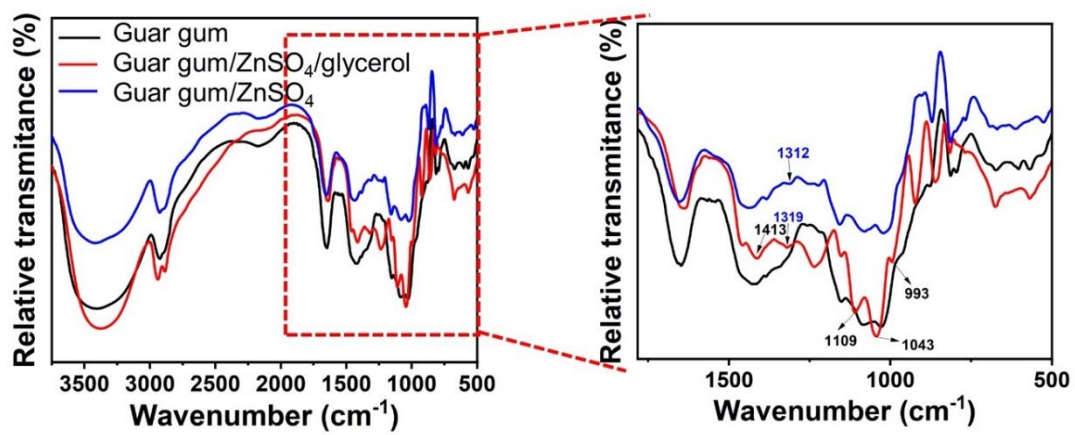


Figure S7 FTIR spectra of different guar gum-based electrolytes. The electrolytes are guar gum, guar gum/ZnSO<sub>4</sub>/glycerol and guar gum/ZnSO<sub>4</sub>, respectively.

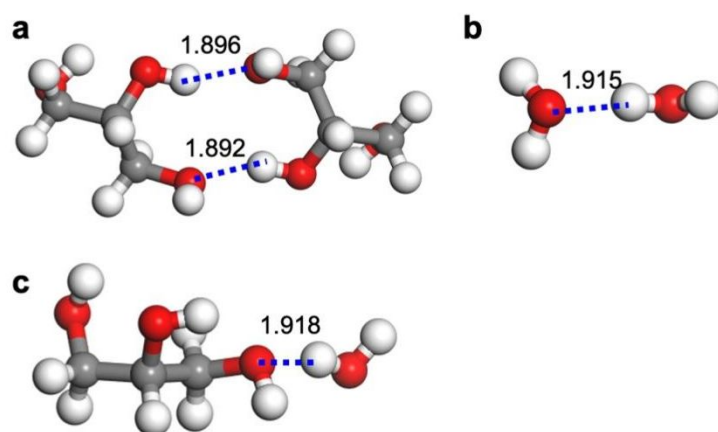


Figure S8 DFT optimized structures via multiple nonbond interactions in the glycerol-water binary hydrogel. (a) glycerol and glycerol (b) H<sub>2</sub>O and H<sub>2</sub>O (c) glycerol and H<sub>2</sub>O.

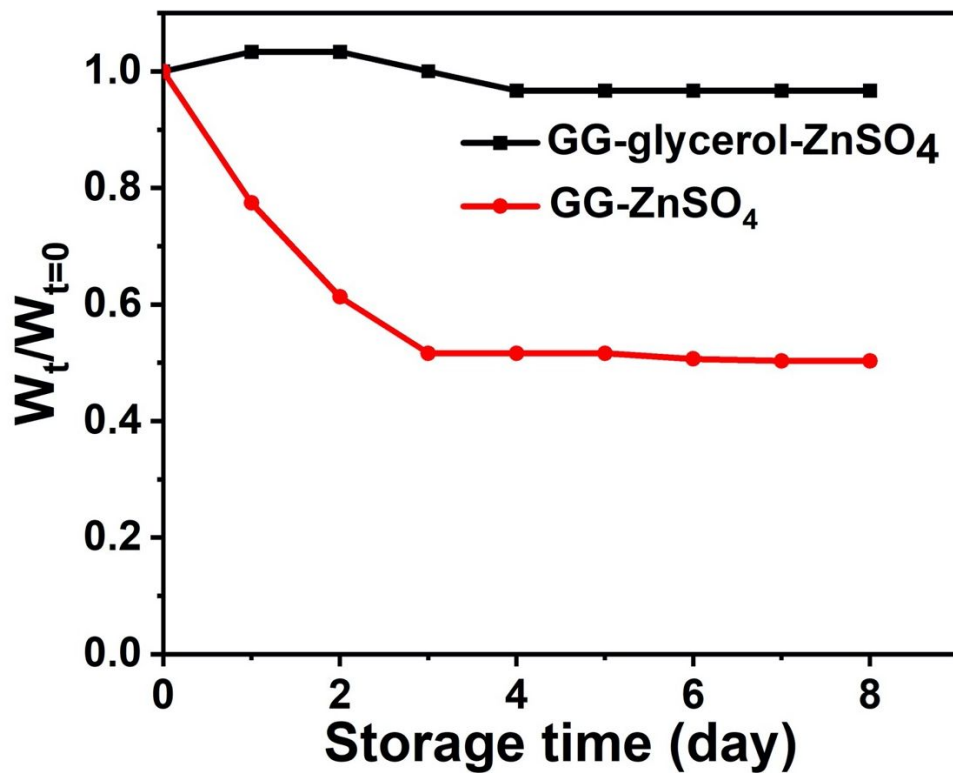


Figure S9 Water-locking capacity of different guar gum-based electrolytes at 25 °C.

The black line represents guar gum/ZnSO<sub>4</sub>/glycerol system and the red line represents guar gum/ZnSO<sub>4</sub> system.

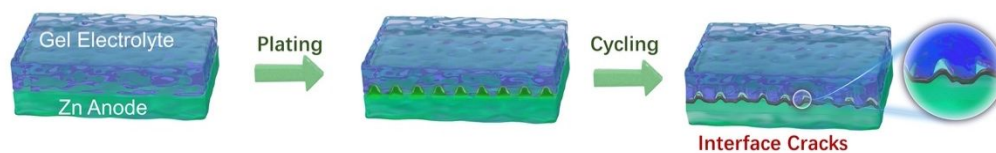


Figure S10 Schematic diagram of the dendrite growth in normal gel batteries. After deep cycling, micro-voids appeared at the interface.

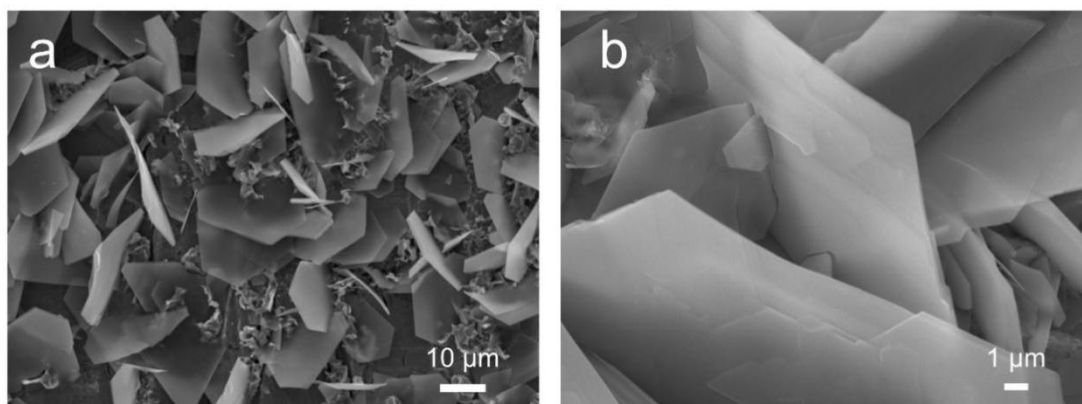


Figure S11 SEM images of zinc anode. The zinc anode was cycled after 250 cycles at  $1 \text{ mA cm}^{-2}$ ,  $1 \text{ mAh cm}^{-2}$  in  $1 \text{ M ZnSO}_4$  aqueous electrolyte with (a) low magnification and (b) high magnification.

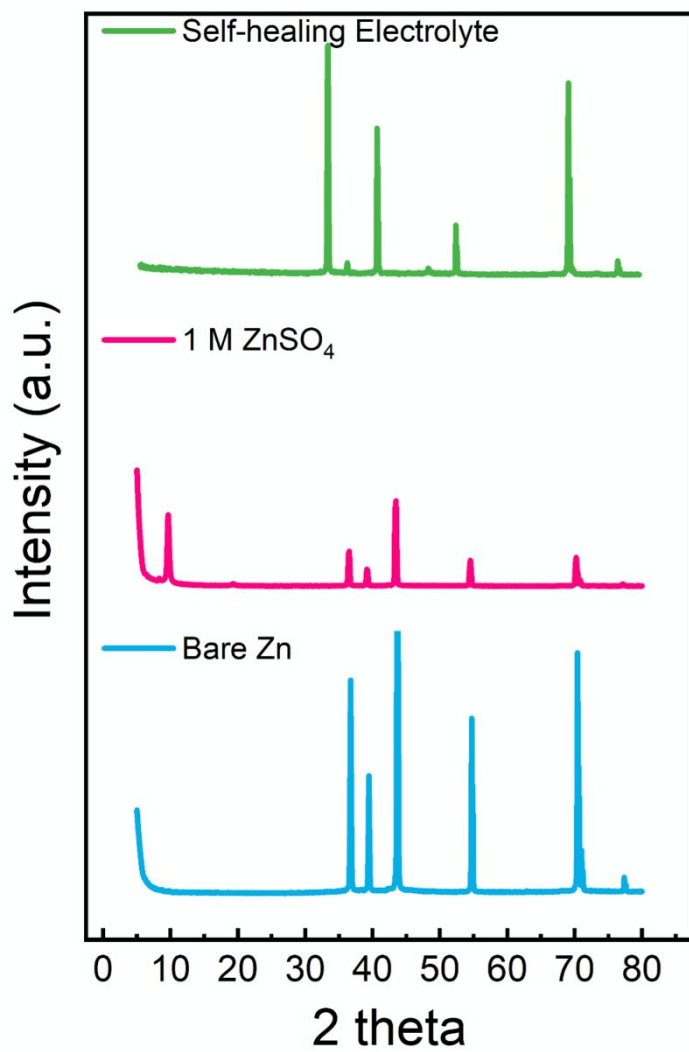


Figure S12 The XRD profiles of different Zn anodes. The Zn anodes are bare Zn, Zn anode after 250 cycles in 1 M ZnSO<sub>4</sub> and Zn anode after 250 cycles in guar gum/ZnSO<sub>4</sub>/glycerol electrolyte at 1 mA cm<sup>-2</sup>, 1 mAh cm<sup>-2</sup>, respectively.

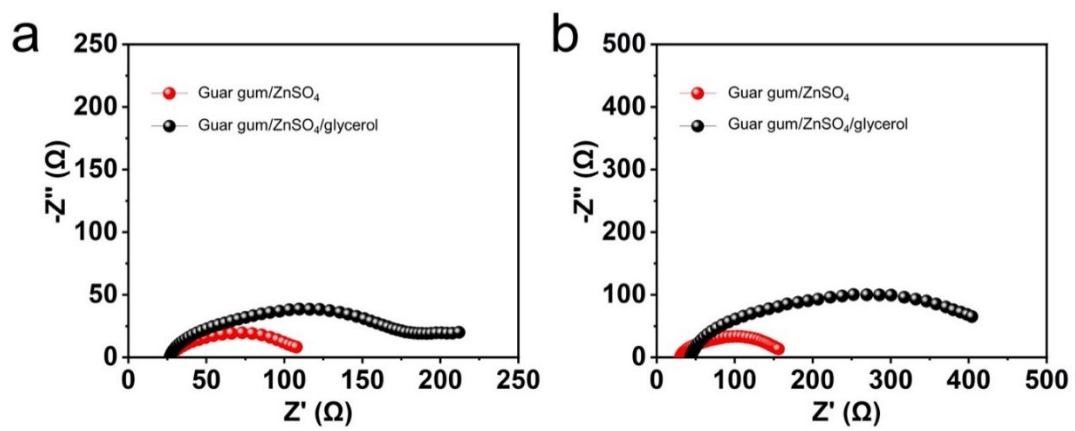


Figure S13 Nyquist impedance plots of the guar gum/ZnSO<sub>4</sub>/glycerol electrolyte and guar gum/ZnSO<sub>4</sub> electrolyte: (a) before cycling and (b) after 250 cycles in the symmetric cells at 1 mA cm<sup>-2</sup>, 1 mAh cm<sup>-2</sup>.

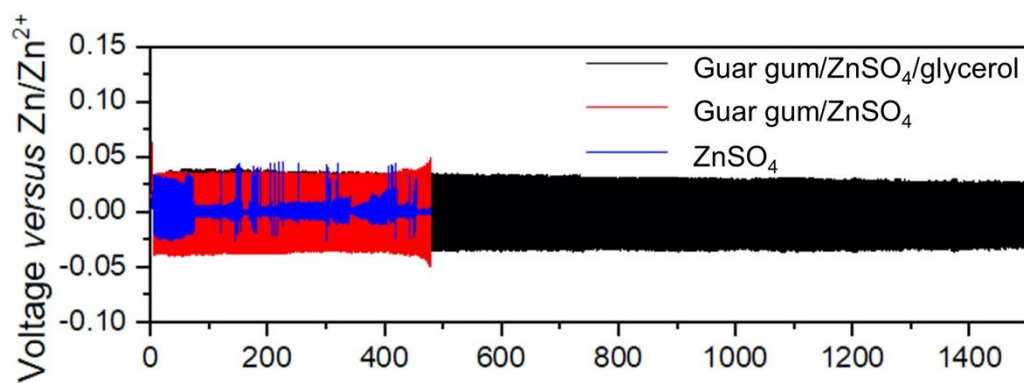


Figure S14 Zn plating/stripping performance in symmetric cells. The Zn//Zn cell were cycled in ZnSO<sub>4</sub>, guar gum/ZnSO<sub>4</sub>/glycerol system and guar gum/ZnSO<sub>4</sub> system at 1 mA cm<sup>-2</sup>, 1 mAh cm<sup>-2</sup>, respectively.

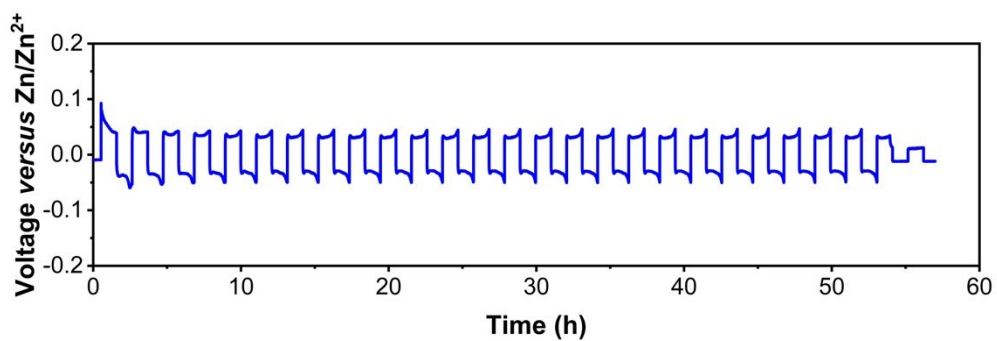


Figure S15 Zn plating/stripping performance in symmetric cell. The Zn//Zn cell was cycled in guar gum/ZnSO<sub>4</sub>/glycerol-0.8 mL system at 10 mA cm<sup>-2</sup>, 10 mAh cm<sup>-2</sup>. Among them, the content of glycerol is 0.8 mL.

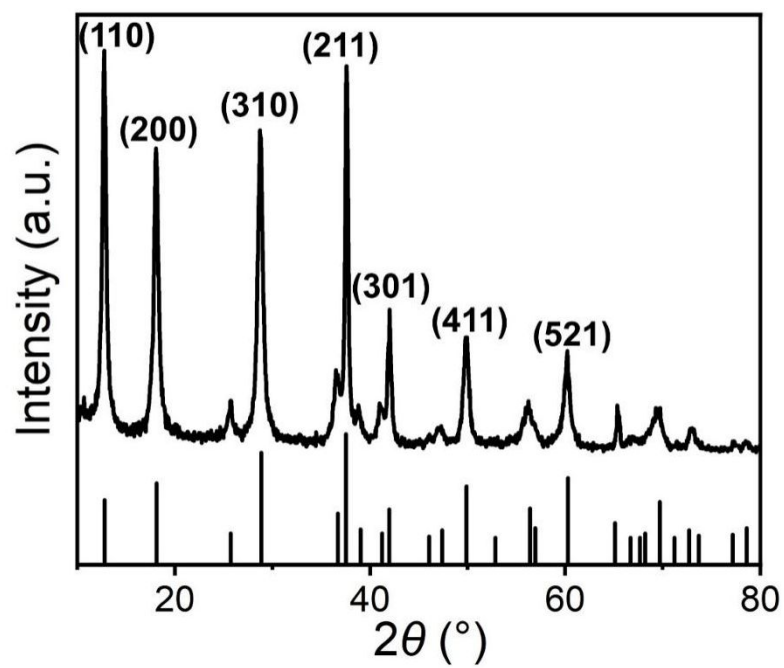


Figure S16 XRD pattern of MnO<sub>2</sub> cathode material, which index to (110), (200), (310), (211), (301), (411), and (521) planes of the  $\alpha$ -MnO<sub>2</sub>.

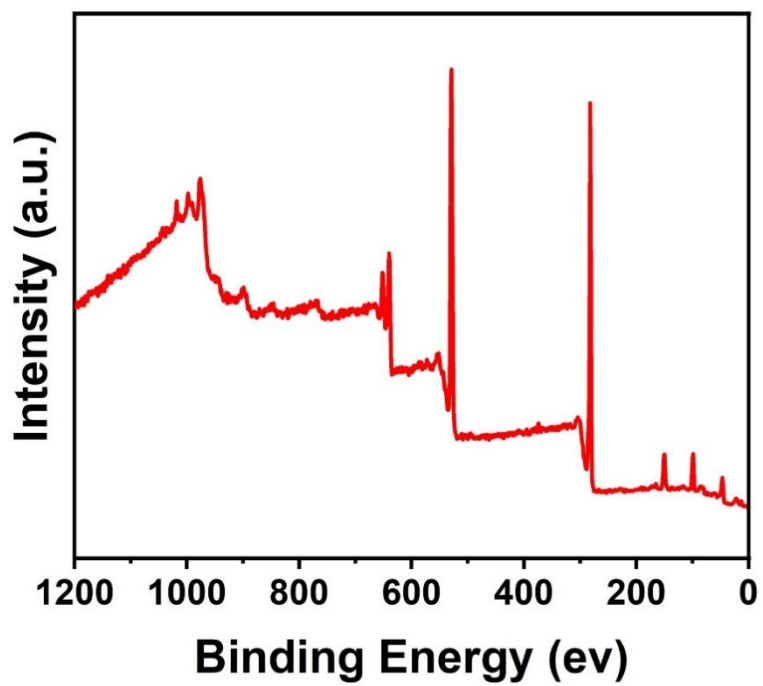


Figure S17 XPS survey spectra of MnO<sub>2</sub> cathode material.

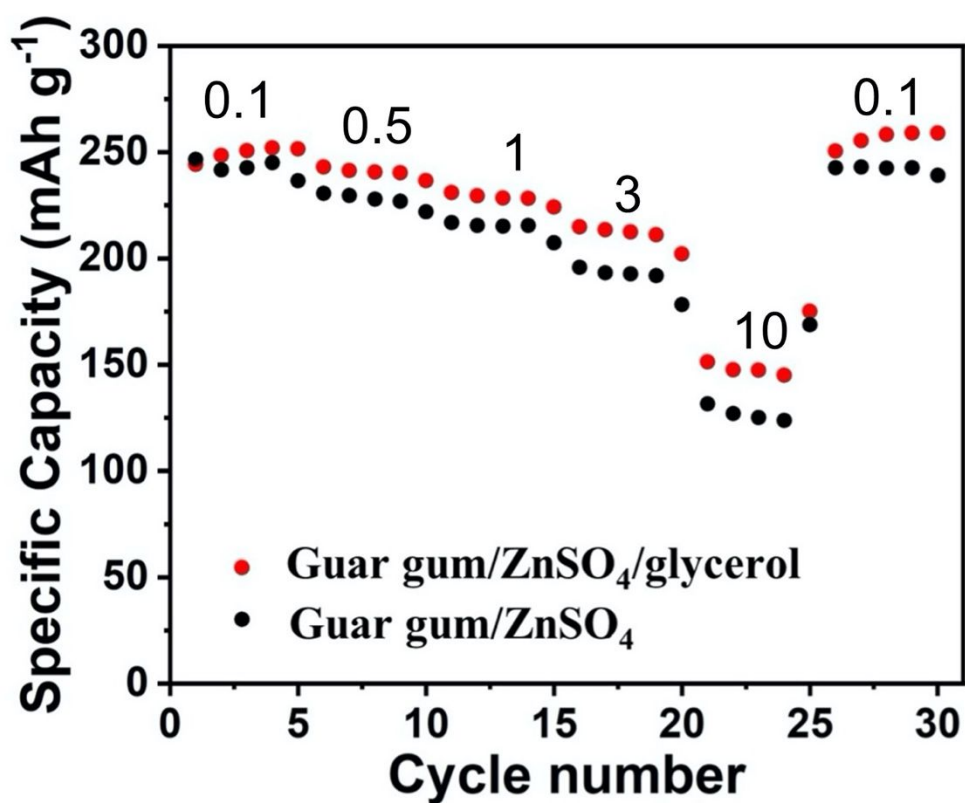


Figure S18 Rate performance of the Zn-MnO<sub>2</sub> full batteries. The Zn//MnO<sub>2</sub> full batteries were cycled in guar gum/ZnSO<sub>4</sub>/glycerol system and guar gum/ZnSO<sub>4</sub> system, respectively. The current densities are 0.1 A g<sup>-1</sup>, 0.5 A g<sup>-1</sup>, 1 A g<sup>-1</sup>, 3 A g<sup>-1</sup>, and 10 A g<sup>-1</sup>, respectively.

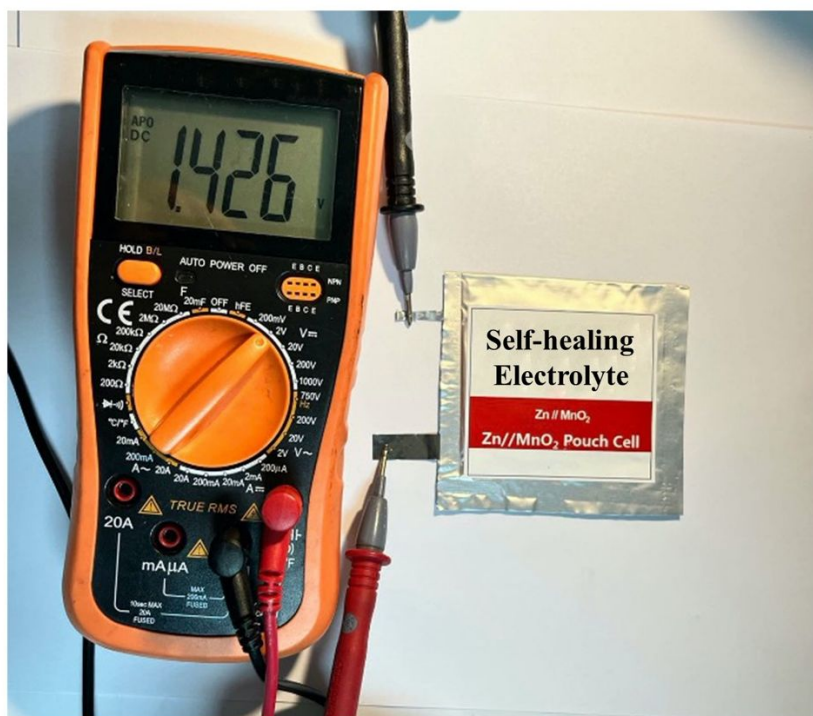


Figure S19 Optical image of the self-healing Zn-MnO<sub>2</sub> pouch cell. The open circuit voltage is 1.426 V and the electrolyte is guar gum/ZnSO<sub>4</sub>/glycerol self-healing gel.

## References for the Supporting Information

- (1) Cox, J.; Singh, M.; Gumbs, G.; Anton, M.; Carreno, Publisher's Note: Dipole-dipole interaction between a quantum dot and a graphene nanodisk. *Phys. Rev. B*, **2013**, *87*, 079903.
- (2) Frisch, M. J.; Trucks, G. W.; Schlegel, H. B.; Scuseria, G. E.; Robb, M. A.; Cheeseman, J. R.; Scalmani, G.; Barone, V.; Mennucci, B.; Petersson, G. A., *Gaussian 09, Revision A.1*, **2009**.
- (3) Wang, Y. L.; Shah, F. U.; Glavatskih, S.; Antzutkin, O. N.; Laaksonen, A. J. J. o. P. C. B., Atomistic insight into orthoborate-based ionic liquids: force field development and evaluation. *J. Phys. Chem. B*, **2014**, *118*, 8711-8723.
- (4) Mja, A.; Tm, D.; Rsb, C.; Sp, A.; Jcsb, C.; Bh, A.; Ela, D. J. S., GROMACS: High performance molecular simulations through multi-level parallelism from laptops to supercomputers. *SoftwareX*, **2015**, *1*, 19-25.